Cell Stem Cell
Short Article

mTOR Complex 1 Plays Critical Roles in Hematopoiesis and *Pten*-Loss-Evoked Leukemogenesis

Demetrios Kalaitzidis,[1] Stephen M. Sykes,[2] Zhu Wang,[1] Natalie Punt,[1] Yuefeng Tang,[3] Christine Ragu,[2] Amit U. Sinha,[1] Steven W. Lane,[4] Amanda L. Souza,[5] Clary B. Clish,[5] Dimitrios Anastasiou,[6,7] D. Gary Gilliland,[8] David T. Scadden,[2] David A. Guertin,[3,*] and Scott A. Armstrong[1,*]

[1]Division of Hematology/Oncology, Children's Hospital Boston and Dana-Farber Cancer Institute, Harvard Medical School and the Harvard Stem Cell Institute, Boston, MA 02115, USA
[2]Department of Stem Cell and Regenerative Biology, Center for Regenerative Medicine, Massachusetts General Hospital, Harvard Medical School and the Harvard Stem Cell Institute, Boston, MA 02114, USA
[3]Program in Molecular Medicine, University of Massachusetts Medical School, Worcester, MA 01605, USA
[4]Queensland Institute of Medical Research, Brisbane 4006, Australia
[5]Metabolite Profiling Initiative, Broad Institute of MIT and Harvard, Cambridge, MA 02142, USA
[6]Department of Medicine, Division of Signal Transduction, Beth Israel Deaconess Medical Center, Boston, MA 02215, USA
[7]Department of Systems Biology, Harvard Medical School, Boston, MA 02115, USA
[8]Division of Hematology, Department of Medicine, Brigham and Women's Hospital, Harvard Medical School, Boston, MA 02115, USA
*Correspondence: david.guertin@umassmed.edu (D.A.G.), scott.armstrong@childrens.harvard.edu (S.A.A.)
http://dx.doi.org/10.1016/j.stem.2012.06.009

SUMMARY

The mechanistic target of rapamycin (mTOR) pathway serves as a key sensor of cellular-energetic state and functions to maintain tissue homeostasis. Hyperactivation of the mTOR pathway impairs hematopoietic stem cell (HSC) function and is associated with leukemogenesis. However, the roles of the unique mTOR complexes (mTORCs) in hematopoiesis and leukemogenesis have not been adequately elucidated. We deleted the mTORC1 component, regulatory-associated protein of mTOR (*Raptor*), in mouse HSCs and its loss causes a nonlethal phenotype characterized by pancytopenia, splenomegaly, and the accumulation of monocytoid cells. Furthermore, *Raptor* is required for HSC regeneration, and plays largely nonredundant roles with rapamycin-insensitive companion of mTOR (*Rictor*) in these processes. Ablation of *Raptor* also significantly extends survival of mice in models of leukemogenesis evoked by *Pten* deficiency. These data delineate critical roles for mTORC1 in hematopoietic function and leukemogenesis and inform clinical strategies based on chronic mTORC1 inhibition.

INTRODUCTION

mTOR is a serine/threonine(Ser/Thr)-protein kinase that has been implicated in regulating key processes in hematopoiesis (Warr et al., 2011). The mTOR pathway is activated under conditions of favorable nutrient availability and directly regulates several downstream metabolic processes, such as mRNA translation, lipid biosynthesis, autophagy, and mitochondrial biogenesis. mTOR exists in two independent multiprotein-containing complexes that have distinct functions in embryonic development and in adult tissue. mTORC1 and mTORC2 are defined by the scaffolding/substrate-guiding proteins Raptor and Rictor, respectively (Laplante and Sabatini, 2012).

Perturbation of the mTOR pathway in adult HSCs of mice, either by the introduction of loss-of-function alleles of *Pten* or *Tsc1* (both negative regulators of mTOR [Laplante and Sabatini, 2012]) or gain-of-function mutations in mTOR activators RHEB2 or AKT, results in HSC cycling and depletion of long-term (LT) reconstituting activity (Yilmaz et al., 2006; Zhang et al., 2006; Chen et al., 2008; Gan et al., 2008; Campbell et al., 2009; Kharas et al., 2010). Chronic mTOR activation can evoke myeloproliferative neoplasms (MPN), and in some cases acute leukemias, suggesting a differential requirement for mTOR between HSCs and leukemia stem cells (LSCs). Furthermore, pharmacological inhibition of mTOR with rapamycin can restore HSC activity and/or deplete LSC function in these models. These studies strongly implicate a role for chronic mTOR activity in HSC and LSC functions, but do not directly address the required roles of the individual mTORCs in these systems. In particular, it is now appreciated that rapamycin is only a partial mTORC1 antagonist (Choo et al., 2008; Hsu et al., 2011; Yu et al., 2011) and can inhibit mTORC2 activity in some cell types (Sarbassov et al., 2006). As ATP-competitive inhibitors of mTOR have recently been demonstrated to have more potent antileukemic activity than rapamycin in leukemias (Janes et al., 2010), knowledge of which mTORC to target to enhance therapeutic index would be of value in developing novel therapeutic interventions. To determine the roles of the mTORCs in hematopoiesis and leukemogenesis, we utilized mice containing conditional loss-of-function alleles for *Raptor* and *Rictor*. We observe that *Raptor* is required for HSC regeneration under stress conditions while not absolutely required during homeostasis, and that *Raptor* and *Rictor* play largely nonredundant roles in these processes. Of note, loss of *Raptor* prolongs

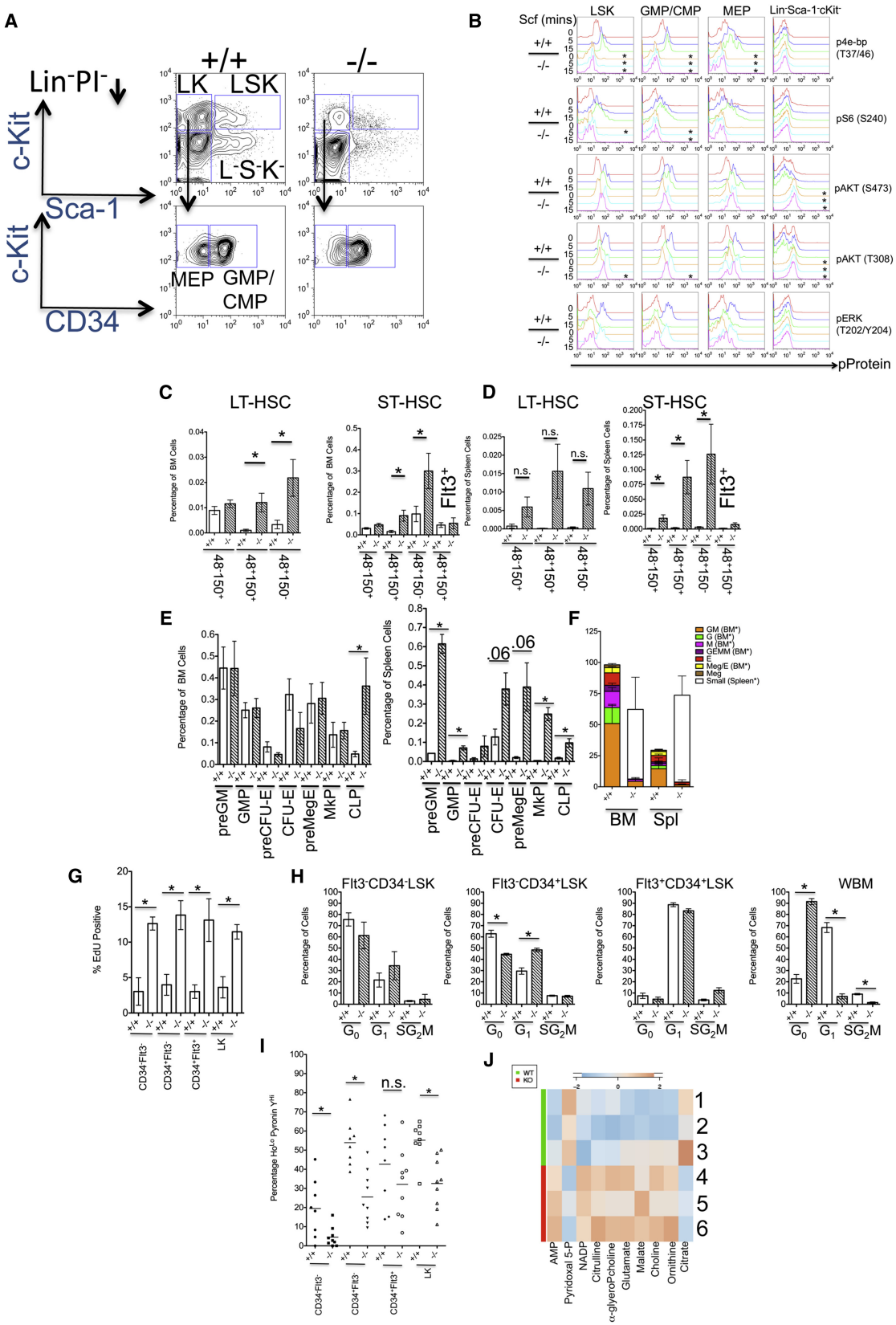
A
+/+
-/-
Lin-PI-
c-Kit
Sca-1
LK
LSK
L-S-K-
c-Kit
CD34
MEP
GMP/
CMP
B
Scf (mins)
LSK
GMP/CMP
MEP
Lin-Sca-1-cKit-
+/+
-/-
p4e-bp (T37/46)
pS6 (S240)
pAKT (S473)
pAKT (T308)
pERK (T202/Y204)
pProtein
C
LT-HSC
ST-HSC
Percentage of BM Cells
Flt3+
48-150+
48+150+
48+150-
D
LT-HSC
ST-HSC
Percentage of Spleen Cells
n.s.
E
Percentage of BM Cells
Percentage of Spleen Cells
preGM
GMP
preCFU-E
CFU-E
preMegE
MkP
CLP
F
GM (BM+)
G (BM+)
M (BM+)
GEMM (BM+)
E
Meg/E (BM+)
Meg
Small (Spleen+)
BM
Spl
G
% EdU Positive
CD34+Flt3-
CD34+Flt3+
CD34+Flt3+
LK
H
Flt3-CD34-LSK
Flt3-CD34+LSK
Flt3+CD34+LSK
WBM
Percentage of Cells
G0
G1
SG2M
I
Percentage Ho-Lo Pyronin Y-Hi
n.s.
J
WT
KO
AMP
Pyridoxal 5-P
NADP
Citrulline
α-glyeroPcholine
Glutamate
Malate
Choline
Ornithine
Citrate
1
2
3
4
5
6

survival of mice in models of leukemogenesis evoked by *Pten* deficiency. These data clarify the roles of the mTORCs in benign and malignant hematopoiesis, while indicating potential deleterious responses due to chronic mTORC1 inhibition in the hematopoietic system.

RESULTS

Deletion of Raptor in Hematopoietic Stem and Progenitor Cells Ablates mTORC1 Activity

We investigated the effects of mTORC1 loss in hematopoiesis by utilizing mice containing *loxP* sites flanking (*floxed [Fl]*) exon 6 of the *Raptor* gene, which upon Cre recombinase expression produce null *Raptor* alleles (Sengupta et al., 2010; Peterson et al., 2011). We conditionally deleted *Raptor* alleles through use of interferon-inducible transgenic *Mx1Cre* mice, in which recombination is induced upon receiving administration of polyinosinic-polycytidylic acid (pIpC) (Kühn et al., 1995). Injection of pIpC into 4- to 8-week-old *Raptor*$^{Fl/+}$, *MxCre* or *Raptor*$^{Fl/Fl}$, *MxCre* mice resulted in efficient deletion of *Raptor* allele(s) and diminished mRNA and protein expression compared with controls (Figures S1A–S1D available online and data not shown). Deletion of *Raptor* in hematopoietic stem and progenitor cells (HSPCs) led to decreased basal and Scf-stimulated levels of phospho(p)-4e-bp, as well as Scf-stimulated levels of pS6 (Figures 1A and 1B; for quantification see Figure S1E). Since mTORC1 inhibition can evoke increased AKT phosphorylation (due to the negation of a negative feedback loop) (Carracedo and Pandolfi, 2008), we also examined pAKT levels in HSPCs. Although phosphorylation at Ser473 was normal in *Raptor* null HSPCs, phosphorylation of AKT at Thr308 was slightly prolonged in Scf-stimulated *Raptor* null LSK and granulocyte/monocyte progenitors and common myeloid progenitors (GMPs/CMPs) (Figure 1B). Strikingly, relative basal levels of pAKT at either site in the more mature Lin$^-$Sca-1$^-$c-Kit$^-$ cells were markedly elevated in *Raptor* null cells, indicating cell type specificity in the mTORC1-PI3K feedback loop in hematopoietic cells (Figure 1B). Levels of pERK were not different between control and *Raptor*-deleted HSPCs, indicating that *Raptor* deletion does not disrupt all c-Kit signaling (Figure 1B).

mTORC1 Regulates Differentiation Along Multiple Hematopoietic Lineages

Raptor null mice were viable, surviving at least 20 months post-pIpC and containing predominately deleted alleles (data not shown). However, within 1 month of deletion, 100% of mice developed a persistent and rapid pancytopenia, splenomegaly with extramedullary hematopoiesis and disrupted splenic architecture, and decreased thymic mass (Figures S1F, S1G, S1K, and S1L and data not shown). Despite the pancytopenia, *Raptor*-deleted bone marrow (BM) maintained BM cellularity (Figures S1G and S1K). However, *Raptor*-deleted BM did show signs of defective hematopoiesis with emergence of monocytoid features (Figures S1G, S1H, and S1I), but without evidence of dysplasia or progression to leukemia in old age (data not shown). *Raptor* loss leads to an accumulation of Mac-1$^+$Gr-1$^{Mid/Lo}$ monocytes as early as 2 weeks and persisting to at least 5–7 months postdeletion (Figures S1H–S1J and S1M). *Raptor* deletion resulted in increased levels of B220$^+$IgM$^-$CD43$^+$ proB cells in the BM and decreased levels of B220$^+$IgM^{lo}IgD^{Hi} mature B cells in spleen (Figures S1H, S1I, and S1M and data not shown). Finally, *Raptor* loss perturbed erythroblast frequencies in the BM and spleen (Figures S1H and S1I). Deletion of Raptor alleles via tamoxifen administration in *Raptor*$^{Fl/Fl}$ mice expressing a *UBIQUITIN C* promoter-driven tamoxifen-inducible Cre-estrogen receptor (Cre-ER) (Ruzankin et al., 1997) also led to monocyte expansion (Figure S1M and data not shown), suggesting that the effects observed in the Mx-Cre model were not due to interferon responses.

Ablation of *Raptor* Expands LSK Subsets and Mobilizes HSPCs

Raptor loss evoked a rapid (within 2 weeks), sustained (5–7 months), and pIpC-independent increase in the frequency of several LSK subsets (Figures 1C and 1D and Figures S1N and S1O). In the LT-HSC-enriched Flt3$^-$CD34$^-$LSK subset (Osawa et al., 1996; Christensen and Weissman, 2001; Yang et al., 1995) *Raptor* loss increased the frequency of both BM CD48$^+$CD150$^+$, and CD48$^+$CD150$^-$ cells, while CD48$^-$CD150$^+$ Flt3$^-$CD34$^-$-LT-HSCs (Kiel et al., 2005; Morita et al., 2010) were largely unaffected (Figures 1C and 1D). In the short-term HSC (ST-HSC)-enriched Flt3$^-$CD34$^+$LSK subset, *Raptor*

Figure 1. Deletion of *Raptor* Ablates mTORC1 Activity and Leads to HSPC Perturbations

(A) Representative flow-cytometry plots of sorted Lin$^-$ PI$^-$ cells postfixation and postpermeabilization from pIpC-treated *Raptor*$^{Fl/Fl}$ (+/+) and *Raptor*$^{Fl/Fl}$, *Mx-Cre* (−/−) mice (Lin$^-$ PI$^-$ Sca-1$^+$c-Kit$^+$ [LSK], Lin$^-$ PI$^-$ Sca-1$^-$c-Kit$^+$[LK], Lin$^-$ PI$^-$ Sca-1$^-$c-Kit$^+$CD34$^+$ [GMP/CMP], Lin$^-$ PI$^-$ Sca-1$^-$c-Kit$^+$CD34$^-$ [MEP], and Lin$^-$ PI$^-$ Sca-1$^-$c-Kit$^-$ [L$^-$ S$^-$ K$^-$]).

(B) Flow cytometry was performed on sorted Lin$^-$PI$^-$ cells from pIpC-treated *Raptor*$^{Fl/Fl}$ (+/+) and *Raptor*$^{Fl/Fl}$, *Mx-Cre* (−/−) mice that were stimulated ex vivo with 20 ng/ml of Scf for the indicated time points in minutes (mins), and these were then processed for flow cytometry. Representative histograms are shown (percent maximal value on the y axis), and for quantification see Figure S1E (*$p < 0.05$ relative to unstimulated +/+ controls).

(C) Quantification of CD48/CD150/CD34/Flt3/LSK subsets from BM and spleen (D) of *Raptor*$^{Fl/Fl}$ (+/+) and *Raptor*$^{Fl/Fl}$, *Mx-Cre* (−/−) mice 5–7 months post-pIpc. (n = 5 +/+, n = 6 −/−.) For gating see Figure S1N.

(E) Quantification of immunophenotypic HPC subsets from mice described in (C), from BM (left panel), and from spleen (right panel). Immunophenotypes are defined as in Pronk et al. (2007).

(F) Colony-forming cell (CFC) formation from pIpC-treated *Raptor*$^{Fl/Fl}$ (+/+) and *Raptor*$^{Fl/Fl}$, *Mx-Cre* (−/−) mouse BM and spleen cells. (n = 3–4.)

(G) Assessment of EdU incorporation in cells from pIpC-treated *Raptor*$^{Fl/Fl}$ (+/+) and *Raptor*$^{Fl/Fl}$, *Mx-Cre* (−/−) mice. (n = 3.)

(H) Ho 33342/Ki67 staining from the indicated FACS-sorted LSK populations or whole BM (WBM) and pIpC-treated genotypes. G_0 (2N DNA-Ki67^{Lo}), G_1 (2N DNA-Ki67^{Hi}), and SG_2M (>2N DNA-Ki67^{Hi}) are shown (n = 3).

(I) Ho 33342/Pyronin Y in the indicated surface-stained populations of the indicated genotypes (as in B) by flow cytometry). Ho^{Lo} = 2N DNA. (n = 8–9.)

(J) Heat-map of metabolite measurements from pIpC-treated *Raptor*$^{Fl/Fl}$ (WT [1–3]) and *Raptor*$^{Fl/Fl}$, *Mx-Cre* (KO [4–6]) LSK cells. ($p < 0.057$, citrate $p = 0.077$.)

All data are expressed as mean or mean ± SEM (*$p < 0.05$, n.s. $p > 0.05$).

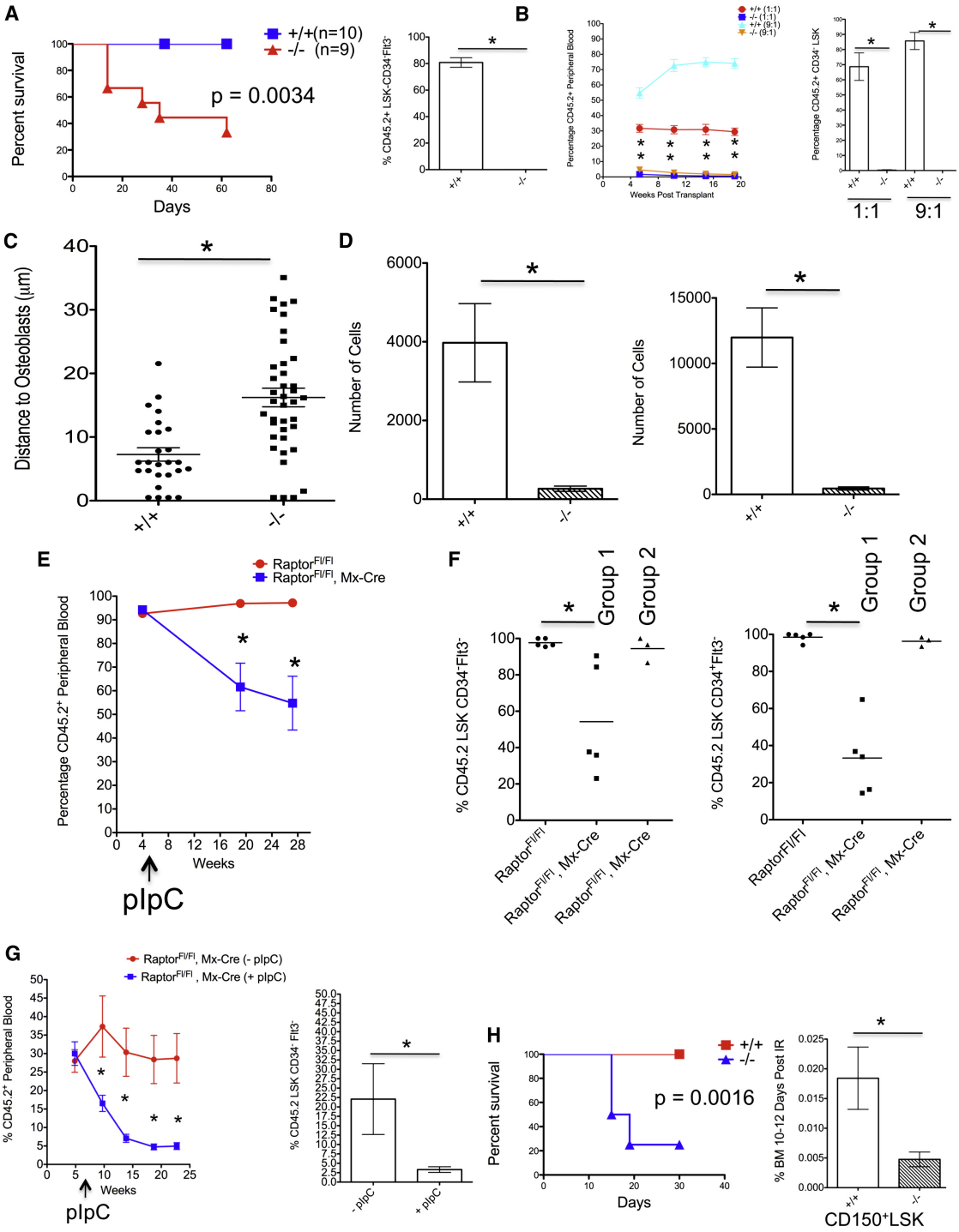

Figure 2. *Raptor* Is Required for HSC Regeneration in a Cell Autonomous Manner

(A) 8 × 10^5 whole BM cells from pIpC-treated *Raptor*$^{Fl/Fl}$ (+/+) or *Raptor*$^{Fl/Fl}$, *Mx-Cre* (−/−) mice (both CD45.2$^+$) were transplanted into lethally irradiated CD45.1 mice and survival was monitored. Numbers of recipient mice are indicated (left panel). (p value was derived by log-rank test). BM from surviving mice was analyzed for CD45.2 cell contribution to the CD34$^-$Flt3$^-$LSK pool 20 weeks post-pIpC (n = 3) (right panel).

(B) BM cells from *Raptor*$^{Fl/Fl}$ (+/+) and *Raptor*$^{Fl/Fl}$, *Mx-Cre* (−/−) mice, 6 weeks post-pIpC treatment (both CD45.2+), were mixed at the indicated ratios with CD45.1$^+$ BM cells and transplanted into lethally irradiated CD45.1 recipients. Percentage of CD45.2$^+$ cells in PB is shown over time (n = 5) (left panel). Twenty-two weeks posttransplantation the percentage of CD45.2$^+$ CD34$^-$LSK cells in BM was assessed (n = 5) (right panel).

(C) FACS-sorted DiD-labeled LSK-CD48$^-$CD150$^+$ from pIpC-treated *Raptor*$^{Fl/Fl}$ (+/+) and *Raptor*$^{Fl/Fl}$, *Mx-Cre* (−/−) mice were transplanted into lethally irradiated Col2.3GFP mice, and ~24 hr later live imaging was performed to assess relative distance of HSPCs to osteoblasts. Shown are results from two independent experiments performed with 5,000–10,000 HSPCs.

loss produced an increase in the frequency of BM $CD48^+CD150^+$, $CD48^+CD150^-$ cells, as well as an increase in $CD48^+CD150^+$-$Flt3^-CD34^+$ LSK cells in the spleen (Figures 1C and 1D). *Raptor* deletion led to an expansion of several splenic $Lin^-c\text{-}Kit^+\text{-}Sca\text{-}1^-$-(LK) subsets (Figure 1E), consistent with increased splenic LSK cells and extramedullary hematopoiesis. While *Raptor* deletion did not affect BM progenitor frequencies, ex vivo colony-forming activity was severely compromised, forming mostly small irregular colonies in complete-cytokine media, which was also observed with total splenocytes (Figure 1F).

Raptor Loss Affects the Cell Cycle and Induces Metabolic and Gene Expression Alterations in HSPCs

To investigate the effects of *Raptor* loss on HSPC cell cycle, 5-ethynyl-2′-deoxyuridine (EdU) incorporation 2 days postinjection was assessed in HSPCs. LSK subtypes as well as LK cells null for *Raptor* incorporated higher levels of EdU (Figure 1G). Furthermore, *Raptor*-deleted ST-HSCs were more likely to be in the G_1 phase of the cell cycle than controls (Figure 1H). However, *Raptor*-deleted LT-HSCs did not show steady-state cell cycle differences, and neither did $Flt3^+CD34^+$LSKs (Figure 1H). Moreover, whole BM cells from *Raptor* null mice were in the G_0 phase of the cell cycle (Figure 1H). We did not detect differences in either caspase activity or reactive oxygen species levels due to *Raptor* loss (data not shown). *Raptor*-deleted LSK subsets, as well as LK cells, did show lower levels of RNA (based on Pyronin Y staining) (Figure 1I). To ascertain other metabolic perturbations caused by *Raptor* loss in HSPCs, we performed metabolite profiling on LSK cells. This analysis revealed elevated intracellular concentrations of AMP and NADP+ in *Raptor* null cells, indicative of effects in energy and redox homeostasis, respectively, and increased levels of intermediates involved in lipid metabolism (choline and α-glycerophosphocholine). We also observed diminished levels of pyridoxal 5′-phosphate, a key cofactor in transamination reactions and other metabolites involved in nitrogen metabolism (citrulline, ornithine, and glutamate) (Figure 1J).

Finally, we assessed gene expression alterations induced by *Raptor* loss in HSPC-enriched $Flt3^-$LSK cells. Gene set enrichment analysis indicated multiple changes in *Raptor* null HSPCs, including alterations in known mTOR-regulated pathways or processes such as cholesterol biosynthesis and the hypoxia inducible factor pathway, as well as potentially novel mTORC1-regulated pathways (i.e., depletion of NUP98-HOXA9 target genes) (Table S1). When considered collectively, these data indicate that under homeostatic conditions, mTORC1 is not absolutely required for HSC maintenance, but its loss does lead to HSPC mobilization and evokes significant cell cycle, metabolic, differentiation, and gene expression changes.

Raptor Is Required for HSC Function Posttransplantation

We next assessed the role of Raptor in hematopoietic regeneration by transplanting BM marked by $CD45.2^+$ cells from $Raptor^{Fl/Fl}$ or $Raptor^{Fl/Fl}$, $MxCre^+$ mice treated with pIpC (+/+ and −/−, respectively) prior to transplantation into lethally irradiated congenic $CD45.1^+$ B6.SJL mice, and found that most mice receiving *Raptor* null BM did not survive (Figure 2A). We then transplanted cells as above along with whole BM marked as $CD45.1^+$ cells from B6.SJL mice into lethally irradiated $CD45.1^+$ B6.SJL mice at 1:1 and 9:1 test:competitor ratios. Mice transplanted with −/− cells showed minimal engraftment beginning as early as 5 weeks posttransplantation (Figure 2B). We also transplanted splenocytes in the same manner as above, and again found minimal engraftment from *Raptor* null cells (data not shown).

To assess the homing capacity of *Raptor* null HSPCs, LSK-$CD48^-CD150^+$ cells were isolated from pIpC-treated $Raptor^{Fl/Fl}$ or $Raptor^{Fl/Fl}$, $MxCre^+$ mice, labeled with 1,1′-dioctadecyl-3,3,3′,3′-tetramethylindodicarbocyanine (DiD), and transplanted into mice with GFP-expressing osteoblasts (Col2.3-GFP) (Lo Celso et al., 2009). By using live in vivo imaging, we did not observe any obvious defects in homing. *Raptor* null HSPCs, however, did localize further from osteoblast cells (Figure 2C). This could reflect a requirement for mTORC1 in integrating niche signals correctly. In fact, *Raptor* null LT-HSCs or ST-HSCs couldn't initiate and/or sustain ex vivo cultures in serum-free conditions containing niche-secreted factors (Zheng et al., 2011) (Figure 2D). Overexpression of several downstream mTORC1 effectors, as well as potential novel targets (namely *Hoxa9*), could not restore ex vivo growth in the absence of *Raptor*.

(D) Two-hundred LT-HSCs or ST-HSCs from pIpC-treated $Raptor^{Fl/Fl}$ (+/+) and $Raptor^{Fl/Fl}$, *Mx-Cre* (−/−) mice were used to initiate cultures in serum-free conditions that promote HSC expansion ex vivo. Seven to nine days postculture the number of cells was enumerated. Data are from three independent experiments performed in duplicate.

(E) 8×10^5 BM cells from non-pIpC-treated $Raptor^{Fl/Fl}$ or $Raptor^{Fl/Fl}$, *Mx-Cre* mice were transplanted into lethally irradiated CD45.1 recipients. Five weeks posttransplantation mice were injected with three doses of pIpC over 5 days. PB chimerism was assessed by measuring the contribution of $CD45.2^+$ cells over the indicated time (n = 9–10 recipients).

(F) BM from mice from (E) was analyzed for CD45.2 chimerism in $CD34^-Flt3^-$ LSK fractions 25 weeks post-pIpC. $Raptor^{Fl/Fl}$, *Mx-Cre* recipients were separated into two $CD45.2^+$ groups, one with low CD45.2 chimerism that retained deletion (Group 1) and one with high CD45.2 chimerism that escaped deletion (Group 2). (n = 4–5.) (See Figure S2C.)

(G) 2.5×10^5 BM cells from uninduced $Raptor^{Fl/Fl}$, *Mx-Cre* were mixed with 2.5×10^5 CD45.1 cells and transplanted into lethally irradiated CD45.1 recipients. Five to seven weeks posttransplantation one-half of the mice were injected with pIpC as in (D) (+pIpC). Contribution of CD45.2 cells to PB was assessed over the indicated time points. (n = 6–8, left panel.) Recipient BM was analyzed for CD45.2 cell contribution to the $CD34^-Flt3^-$LSK pool 21 weeks post-pIpC (n = 6–8) (right panel).

(H) Kaplan-Meier (KM) survival curve from pIpC-treated $Raptor^{Fl/Fl}$ (+/+), n = 10, and $Raptor^{Fl/Fl}$, *Mx-Cre* (−/−) (n = 4) mice that received sublethal irradiation. The one surviving −/− mouse had escaped deletion (data not shown) (left panel). (p value was derived by log-rank test.) pIpC-treated $Raptor^{Fl/Fl}$ (+/+) and $Raptor^{Fl/Fl}$, *Mx-Cre* (−/−) mice received sublethal irradiation, and shown is the frequency of BM $CD150^+$-LSK cells 10–12 days postirradiation (IR). (n = 4.)

All data are expressed as mean or mean ± SEM (*p < 0.05).

Raptor Is Required Cell Autonomously for HSC Regeneration

To examine the cell autonomous phenotypes, we transplanted BM from non-pIpC-treated *Raptor*$^{Fl/Fl}$ or *Raptor*$^{Fl/Fl}$, *MxCre*$^{+}$ mice (without helper/competitor) into lethally irradiated CD45.1^{+} B6.SJL mice, waited ~5 weeks, and then induced deletion with pIpC. Approximately 1 month post-pIpC treatment, all mice receiving *Raptor*$^{Fl/Fl}$, *MxCre* cells developed leukopenia, while mice receiving *Raptor*$^{Fl/Fl}$ did not (Figure S2A). Furthermore, CD45.2^{+} cells from pIpC-treated mice receiving *Raptor*$^{Fl/Fl}$, *MxCre*$^{+}$ cells were mostly Mac-1^{+}Gr-1$^{Mid/Lo}$ (Figure S2B). After 16 weeks host CD45.1^{+} cells began to contribute substantially to peripheral chimerism only in pIpC-treated mice receiving *Raptor*$^{Fl/Fl}$, *MxCre*$^{+}$ cells (Figure 2E). We then analyzed the BM and spleens of transplant recipients and observed that mice from pIpC-treated *Raptor*$^{Fl/Fl}$, *MxCre*$^{+}$ could be segregated into two groups. One (Group 1) had maintained relatively low percentages of CD45.2^{+} cells in the BM and spleen, and had retained deleted-*Raptor* alleles, whereas the other (Group 2) contained a high percentage of CD45.2^{+}, but contained mostly floxed *Raptor* alleles (i.e., they had escaped deletion) (Figure S2C). This differential chimerism was also observed in LT-HSC and ST-HSC fractions (Figure 2F), suggesting a cell autonomous role for Raptor in HSC self-renewal. Finally, we transplanted BM cells from *Raptor*$^{Fl/Fl}$, *MxCre*$^{+}$ mice with BM cells from B6.SJL mice at a 1:1 ratio, waited for stable engraftment (~5 weeks), and then induced deletion of *Raptor* alleles in one-half of the mice. Mice receiving pIpC displayed a steady reduction in peripheral chimerism, and *Raptor* null grafts were outcompeted (Figure 2G).

To assess the regenerative capacity of *Raptor* null HSCs in nontransplantation settings, pIpC-treated *Raptor*$^{Fl/Fl}$ (+/+) or *Raptor*$^{Fl/Fl}$, *MxCre*$^{+}$ (−/−) mice were treated with a sublethal dose of irradiation. While all +/+ mice survived this treatment and showed signs of BM regeneration over time, most −/− died rapidly, without signs of normal BM regeneration (Figure 2H and data not shown). Furthermore, while +/+ LT-HSC enriched CD150^{+}-LSK cells were reduced by 5.8 ± 1.3-fold relative to unirradiated mice 10–12 days postirradiation, there was a 16.9 ± 3.7-fold decrease in this population in −/− mice ($p < 0.05$) (Figure 2H). Taken together, these data indicate that Raptor/mTORC1 activity appears to be generally required in regenerative hematopoietic settings.

Neither mTOR Complex Is Absolutely Required In Hematopoietic Homeostasis

To determine the role of mTORC2 in adult hematopoiesis, we utilized mice with a floxed *Rictor* exon 3 allele (Shiota et al., 2006) and generated *Rictor*$^{Fl/Fl}$ or *Rictor*$^{Fl/Fl}$, *MxCre*$^{+}$ animals. pIpC treatement of *Rictor*$^{Fl/Fl}$, *MxCre*$^{+}$ mice ablated mTORC2 activity in HSPC in response to Scf, but did not affect phosphorylation of AKT at Thr308 or mTORC1 activity (Figure 3A). Deletion of *Rictor* in the hematopoietic system was tolerated and primarily resulted in diminished peripheral blood (PB) lymphocytes, a reduction in spleen mass, and a decrease in splenic B220^{+} IgM^{Lo}IgD^{+} cells (Figures S3A–S3C and data not shown), phenotypes consistent with loss of PI3K/AKT signaling (Fruman et al., 1999; Calamito et al., 2010). *Rictor* loss did not affect HSPC number by immunophenotype (Figure 3B and data not shown) and did not diminish HSPC chimerism at 30 weeks in a competitive transplant (Figure 3C). However, we did observe that *Rictor* null BM contributed to lower levels of PB cells, particularly those of the lymphoid lineages (Figure 3C and Figure S3D).

Finally, we assessed the requirement of both mTORC1 and mTORC2 in hematopoietic homeostasis by generating compound *Raptor*$^{Fl/Fl}$, *Rictor*$^{Fl/Fl}$, *MxCre*$^{+}$. pIpC-treatment of *Raptor*$^{Fl/Fl}$, *Rictor*$^{Fl/Fl}$, *MxCre*$^{+}$ led to reduced phosphorylaton of both mTORC1 and mTORC2 substrates in HSPCs (Figure 3D).

Compound-deleted mice had phenotypes largely resembling hematopoietic *Raptor* deletion, and did not develop BM failure (Figures 3E and 3F and Figures S3E–S3I and data not shown) (Figure 3E). Lastly, compound mice retained deleted alleles of both *Raptor* and *Rictor* up to 10 months postdeletion (data not shown). Taken together, mTORC1 and/or mTORC2 play largely nonredundant roles in hematopoiesis.

Raptor Deletion Prolongs Survival in Models of *Pten*-Loss-Evoked Leukemogenesis

Since hyperactivation of mTOR is observed in many hematological malignancies (Chapuis et al., 2010), we asked whether complete loss of function of mTORC1 could impact leukemogenesis in vivo. We utilized *Pten*$^{Fl/Fl}$, *MxCre* mice that develop symptoms of myeloproliferative neoplasm (MPN), can progress to acute leukemia, and whose leukemias are sensitive to rapamycin (Yilmaz et al., 2006; Zhang et al., 2006). We produced *Pten*$^{Fl/Fl}$ mice that were *Raptor*$^{+/+}$, *Raptor*$^{Fl/+}$, or *Raptor*$^{Fl/Fl}$ (all *MxCre* positive) and induced deletion. Homozygous, but not heterozygous, *Raptor* deletion significantly prolonged survival of *Pten* null mice, and ameliorated some but not all neoplasia-associated phenotypes (Figures S4B–S4E). However, homozygous *Pten* deletion did lead to lethality in the majority of compound mice (Figure 4A). Surviving doubly-deleted mice displayed slightly enlarged spleens and significantly larger livers relative to induced *Raptor*$^{Fl/Fl}$, *MxCre* mice (532 ± 83.8 versus 318 ± 37.72 mg for spleen weights, $p < 0.05$, and 2.44 ± .347 versus 1.16 ± 0.113 g for liver weights, $p < 0.05$, $n = 4–6$). White blood cell (WBC) liver infiltrates were apparent in some animals, while some animals displayed large amounts of liver lipid deposits (data not shown). Efficient deletion in most cells for both *Raptor* and *Pten* alleles was detected (Figure 4B and Figure S4A). Finally, *Raptor* loss had no effect on the frequency of *Pten*-loss-evoked changes to BM or splenic LSK-CD48^{-}CD150^{+} cells (Figure 4C).

To investigate if these effects were cell autonomous, we transplanted *Pten*$^{Fl/Fl}$, *MxCre*$^{+}$ cells that were either *Raptor*$^{Fl/+}$ or *Raptor*$^{Fl/Fl}$ (both CD45.2^{+}) along with CD45.1^{+} helper/competitor cells at a 2:1 ratio into B6.SJL mice, waited ~5 weeks for engraftment, and then treated them with pIpC. In this system, most mice receiving *Pten*$^{Fl/Fl}$, *MxCre* BM develop hematological malignancies, the most prevalent of which is T-acute lymphoblastic leukemia/lymphoma (T-ALL) (Lee et al., 2010). Heterozygous deletion of *Raptor* in this model led to a median survival of 11 weeks post-pIpC, while homozygous deletion of *Raptor* only lead to lethality in a few of the transplant recipients (Figure 4E). Notably, after 22 weeks homozygous deletion of *Raptor* lead to reduced chimerism (Figures 4E and 4F). Therefore, *Raptor* is required in a cell autonomous manner for efficient *Pten*-loss-evoked leukemogenesis.

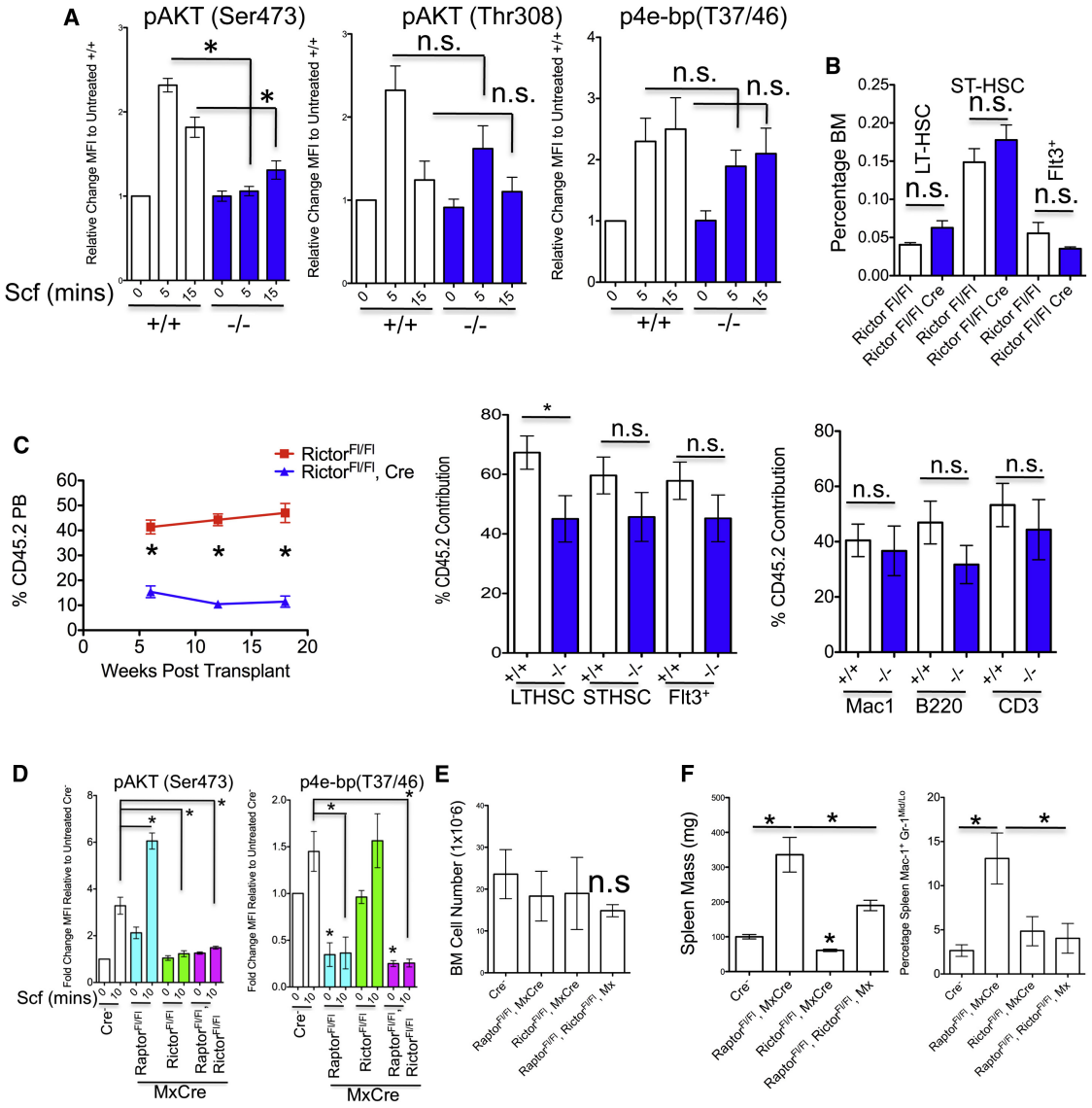

Figure 3. *Rictor* Is Required for mTORC2 Activity in HSPC, but Not LT-Hematopoietic, Regeneration

(A) Flow cytometry was performed on sorted LIN$^-$PI$^-$ cells from pIpC-treated *Rictor*$^{Fl/Fl}$ (+/+) and *Rictor*$^{Fl/Fl}$, *Mx-Cre* (−/−) mice that were treated with Scf for the indicated time (mins). Shown are data from fixed/permeablized LSK-gated events, and fold change in median fluorescent intensity (MFI) for the indicated p-protein is shown relative to untreated +/+ cells. (n = 3–4 mice.)

(B) Frequency of BM LSK subsets from *Rictor*$^{Fl/Fl}$ (+/+) and *Rictor*$^{Fl/Fl}$, *Mx-Cre* (−/−) mice 4 months post-pIpC treatment. (n = 4–5.)

(C) 5 × 10^5 whole BM cells from pIpC-treated *Rictor*$^{Fl/Fl}$ (+/+) and *Rictor*$^{Fl/Fl}$, *Mx-Cre* (−/−) mice (both CD45.2+) were mixed with the same amount of CD45.1$^+$ BM cells and transplanted into lethally irradiated CD45.1 recipients. The percentage of CD45.2$^+$ cells in PB is shown over the indicated time (n = 6–7 recipients). Panels on the right show the percent contribution of CD45.2$^+$ cells to the indicated BM populations 30 weeks posttransplantation. Data are from one of two experiments.

(D) The levels of indicated p-proteins were assessed as in (A) in Scf-treated LSK-gated cells from pIpC-treated mice of the indicated genotypes. (n = 3–4 mice per genotype.)

(E) BM cell number (n = 2–9), spleen mass (F) (n = 5–9), and percentage of Mac-1$^+$Gr-1$^{Mid/Lo}$ splenic cells (F, right panel) (n = 3–5) are shown from mice of the indicated genotype 1–3 months post-pIpC treatment.

All data are expressed as mean ± SEM (*p < 0.05, n.s. p > 0.05).

Although it was diminished, we did observe T cell lymphoma/leukemia development in a minority of *Pten*/*Raptor* double knockouts (that could be transplanted; data not shown). As mTORC2 is functionally active in *Raptor*-deleted cells, we sought to determine the role of mTORC2 in Pten-loss disease in the absence of *Raptor*. We observed the highest levels of AKT phosphorylation at Ser473 in *Raptor*/*Pten* double homozygous-deleted LSK cells (Figure 4G). Hyperactivation of AKT should predictably result in diminished Foxo activity (Guertin et al., 2006), which has previously been associated with depletion

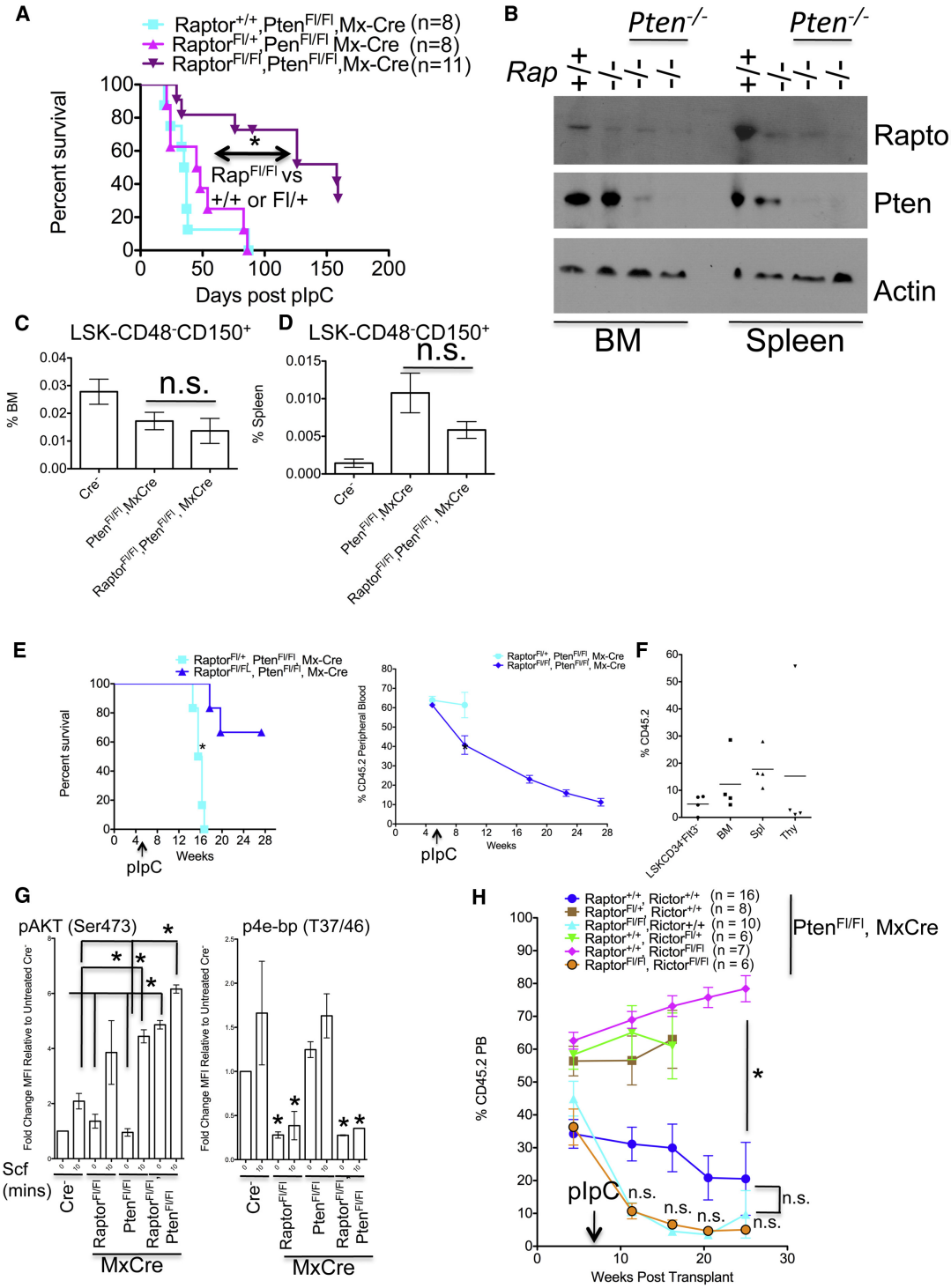

Figure 4. *Raptor* Is Required for Efficient Leukemogenesis Evoked by *Pten* Loss

(A) KM curve from *Pten*$^{Fl/Fl}$, *MxCre* mice of the indicated *Raptor* genotypes that were treated with pIpC. Number of mice is indicated (*$p < 0.05$, log-rank test).

(B) Western blots were performed with BM and spleen extracts from mice of the indicated genotypes ~6 months post-pIpC using the indicated antibodies. Shown are samples from two individual pIpC-treated *Raptor*$^{Fl/Fl}$, *Pten*$^{Fl/Fl}$, *MxCre* mice.

(C) The frequency of BM and splenic (D) LSK-CD48^{-}CD150^{+} cells was assessed from mice of the indicated genotypes 2.5 to 5 weeks post-pIpC treatment (n = 6–10).

(E) 1 × 10^{6} BM cells from non-pIpC-treated mice of the indicated genotypes (CD45.2) were mixed with 5 × 10^{5} CD45.1 cells and transplanted into lethally irradiated CD45.1 mice. Five and one-half weeks posttransplant mice received three injections of pIpC over six days. Survival (left) and chimerism (right) were then assessed (n = 4–6, *$p < 0.05$, log-rank test).

of HSC function (Tothova et al., 2007) as well as impaired leukemogenesis (Sykes et al., 2011). We thus generated *Raptor*$^{Fl/Fl}$, *Rictor*$^{Fl/Fl}$, *Pten*$^{Fl/Fl}$, *MxCre*$^{+}$ triple knockout mice and induced deletion (Figure S4F). However, all triple knockout mice died relatively rapidly (median survival of 19 days [n = 6] without signs of BM failure [data not shown]). We next transplanted non-pIpC-treated BM from *Raptor*$^{Fl/Fl}$, *Rictor*$^{Fl/Fl}$, *Pten*$^{Fl/Fl}$, *MxCre* mice along with controls (Figure 4H) as above, and induced deletion 5–7 weeks posttransplantation. The additional loss of *Rictor* (in the *Raptor*/*Pten* double knockout cells) did not lead to any differences relative to *Raptor*-deleted *Pten*-homozygous chimerism (Figure 4H). Notably, homozygous deletion of *Rictor* alone did allow for stable LT PB chimerism and prolonged survival (Figure 4H and data not shown).

DISCUSSION

We found that Raptor/mTORC1 plays critical functions in HSPCs, hematopoietic differentiation, and leukemogenesis. Previous work has established chronic mTOR activation as depleting HSC function. Herein, we identify mTORC1 to be required for HSC function under regenerative settings. It is likely then that the level of mTORC1 activity needs to be balanced in HSCs, whereas either increased or decreased mTORC1 levels result in diminished capacity for HSC function. As mTOR lies downstream of several hematopoietic growth factor/cytokine receptors, this could reflect a particular need for this signaling axis in self-renewal under regenerative conditions. In fact, thrombopoietin (Thpo), which partially signals through mTOR, has been shown to be essential for HSC function (Qian et al., 2007). Of note, Thpo deficiency evokes similar decreases in several self-renewal-associated *HoxA* genes that are also downregulated in *Raptor* null HSPCs (Table S1). We propose that mTORC1 enables proper HSC sensing of both niche factors and cellular energetic state, and that loss of function of mTORC1 leads to imprecise integration of these signals and loss of regenerative potential.

While loss of *Raptor* leads to multiple hematopoietic abnormalities, homozygous *Raptor* deletion in hematopoietic cells is tolerated in mice, as is complete ablation of both mTORC1 and mTORC2 activity under homeostatic hematopoietic settings. We have demonstrated that mTORC1 loss via homozygous *Raptor* ablation is sufficient to extend survival in mouse models of *Pten*-loss-evoked leukemogenesis in a cell autonomous manner. Previous results have shown that *Pten*-loss-evoked HSC depletion is rapamycin sensitive (Yilmaz et al., 2006). In contrast, our results show that homozygous deletion of *Pten* and *Raptor* leads to a gradual loss in reconstituting capacity (Figure 4D). It is possible that rapamycin-sensitive functions of mTORC1 downstream of *Pten* loss, perhaps the upregulation of the p53/p19^{Arf}/p16^{Ink4a} axis, lead to HSC depletion (Lee et al., 2010), while rapamycin-insensitive functions of mTORC1 are required for HSC regeneration independent of Pten levels. These rapamycin-sensitive functions of mTORC1 are potentially downstream of mTORC2 signaling in response to *Pten* loss. In fact, Magee et al. (2012) demonstrate that loss of *Rictor* extends survival of pIpC-treated *Pten*$^{Fl/Fl}$, *MxCre* mice, while also showing that rapamycin does not affect mTORC2 activity in HSCs in vivo. Unlike some *Raptor*-deleted mice in this setting (MxCre), *Rictor* deletion was not compatible with acute leukemia/lymphoma development. Furthermore, like rapamycin treatment and unlike *Raptor* deletion, *Rictor* deletion restores normal function to *Pten*-deleted HSCs (Magee et al., 2012). When these data are taken together, both mTORC1 and mTORC2 functions appear to be required downstream of *Pten* loss in HSC function as well as in leukemogenesis, while mTORC1 functions appear to be important for HSC regeneration regardless of Pten status.

This work demonstrates previously uncharacterized functions of mTORC1 in hematopoiesis and nonredundant hematopoietic functions of mTORCs, and confirms mTORC1 requirements in cancers with hyperactivation of the PI3K pathway. This work also provides mechanistic insight into the role of specific signaling pathways that control hematopoietic regeneration and will inform on therapeutic strategies.

EXPERIMENTAL PROCEDURES

Mouse Experiments

Mouse strains are detailed in the Supplemental Experimental Procedures. Deletion of floxed alleles was induced by intraperitoneal (IP) injections of 4- to 8-week-old *Mx1Cre* mice with 15 μg/g body weight pIpC three times over 5–6 days, or *UBC-cre-ER* compound mice with 200 μg/g body weight Tamoxifen (Sigma, St. Louis, MO) once daily for 3 days. For transplantation experiments mice received lethal doses of irradiation (two doses at 550 rad 3 hr apart) prior to transplantation of BM cells by retro-orbital injection on the same day. Complete blood counts were performed on PB samples using a Hemavet (Drew Scientific, Dallas, TX).

Flow Cytometry

Antibodies utilized for flow cytometry are detailed in the Supplemental Experimental Procedures. Cells were isolated from BM either by flushing long bones or crushing bones in a mortar and pestle, red blood cells (RBC)s were lysed with BD Pharmlyse lysis buffer (BD), and cells were passed through 40 or 70 μm nylon cell strainers (BD). BM cells used in sorting experiments were enriched for Lin^{-} cells by being stained with PE-Cy5-conjugated rat anti-mouse antibodies, followed by being incubated with sheep anti-rat Dynabeads (Invitrogen, Carlsbad, CA) and undergoing cell separation with magnetic columns. Intracellular flow cytometry was performed as described previously (Kalaitzidis and Neel, 2008). EdU incorporation was assessed by IP injection of mice with 60 mg/kg EdU, and incorporation was analyzed in FACS-sorted cell populations with the Click-iT EdU (Alexa Fluor-647) Assay kit (Invitrogen). For Ki67/DNA staining, FACS-sorted cells were washed once with PBS, resuspended in cold 70% ethanol, and left at −20°C overnight. Cells were pelleted, washed once with 0.5% BSA/PBS, and stained with a PE-Cy7-conjugated antibody to Ki67 (B56 [BD]) and 30 μM Hoechst (Ho) 33342

(F) Chimerism was assessed from surviving mice that received *RaptorFl/Fl, PtenFl/Fl, MxCre* cells from (E), in the indicated cell populations/organs. described in (E). (n = 4.)

(G) Assessment of p-protein levels in LSK-gated events from Scf-treated LIN^{-}PI^{-} cells of the indicated genotypes (n = 2–3).

(H) BM cells from mice of the indicated genotypes (all from *Pten*$^{Fl/Fl}$, *MxCre* backgrounds) were transplanted and treated as in (D). Number of transplant recipients is indicated.

All data are expressed as mean or mean ± SEM (*$p < 0.05$, n.s. $p > 0.05$).

(Invitrogen) for 30 min at 20°C prior to preparation for flow cytometric analysis. For DNA/RNA content measurements, BM cells in 10%FBS/IMDM/50 μg/ml verapamil were incubated with 30 μM Ho 33342 for 45 min at 37°C, washed, and stained for surface markers and 3 μg/mL Pyronin Y (Sigma) for 20 min at 37°C. Enumeration of 200 FACS-sorted LT-HSCs or ST-HSCs grown in 500 μl in wells of 12-well plates, in conditions described previously (Zheng et al., 2011), was with Countbright Absolute Counting Beads (Invitrogen).

Gene Expression Analysis

RNA from FACS-sorted cells was isolated with the Arcturus PicoPure RNA Isolation Kit (Applied Biosystems, Carlsbad, CA). cDNA was synthesized using the High-Capacity cDNA Reverse Transcription Kit (Applied Biosystems). Quantitative PCR was performed using Taqman probes to murine Gapdh and Raptor (Mm00712697_m1 spanning exons 5–6 and Mm01242616_g1 spanning exons 8–9). qPCR reactions were run on either Applied Biosystems 7300 or 7500 RT PCR Systems. Details of microarray experiments are supplied in the Supplemental Experimental Procedures.

Metabolite Profiling

For metabolite profiling BM cells from four mice per genotype were pooled and used to FACS sort 100,000–150,000 LSK cells (one biological replicate). Cells were washed with PBS and resuspended in 200 μl of 100% methanol. Metabolite measurements are from three biological replicates per genotype. A detailed description of the methods used to obtain raw data is in the Supplemental Experimental Procedures.

In Vivo Imaging

In vivo imaging was performed on 5,000–10,000 Vybrant DiD-dye labeled (Invitrogen) LSK-CD48$^-$CD150$^+$ FACS-sorted cells using Col2.3-GFP recipient mice as described previously (Lo Celso et al., 2009) and detailed in the Supplemental Experimental Procedures.

Statistical Analysis

The statistical significance of differences between population means was assessed by two-tailed unpaired Student's t test unless otherwise indicated.

ACCESSION NUMBERS

Microarray data have been deposited at the NCBI Gene Expression Omnibus with accession code GSE32265.

SUPPLEMENTAL INFORMATION

Supplemental Information for this article includes four figures, one table, and Supplement Experimental Procedures and can be found with this article online at http://dx.doi.org/10.1016/j.stem.2012.06.009.

ACKNOWLEDGMENTS

We wish to thank Rebekka Schneider-Kramann for assistance with pathology, Kristina M. Brumme for assistance with mouse husbandry, and Michael G. Kharas for review of the manuscript. D.K. was supported by NIDDK grant K01DK092300; C.B.C. was partially supported by the Nestle Research Center; D.G.G. is currently a full-time employee of Merck and Co. Inc.; D.T.S. was supported by NIH grants HL097794, HL097748, HL100402, and DK050234; D.A.G. was supported by NIH grant R00 CA129613 and the PEW Charitable Trust; and S.A.A. was supported by grants from the Leukemia and Lymphoma Society, The American Cancer Society, The Charles H. Hood Foundation, and NIH grants CA66996, CA105423, and DK049216.

Received: October 5, 2011
Revised: April 10, 2012
Accepted: June 8, 2012
Published: September 6, 2012

REFERENCES

Calamito, M., Juntilla, M.M., Thomas, M., Northrup, D.L., Rathmell, J., Birnbaum, M.J., Koretzky, G., and Allman, D. (2010). Akt1 and Akt2 promote peripheral B-cell maturation and survival. Blood *115*, 4043–4050.

Campbell, T.B., Basu, S., Hangoc, G., Tao, W., and Broxmeyer, H.E. (2009). Overexpression of Rheb2 enhances mouse hematopoietic progenitor cell growth while impairing stem cell repopulation. Blood *114*, 3392–3401.

Carracedo, A., and Pandolfi, P.P. (2008). The PTEN-PI3K pathway: of feedbacks and cross-talks. Oncogene *27*, 5527–5541.

Chapuis, N., Tamburini, J., Green, A.S., Willems, L., Bardet, V., Park, S., Lacombe, C., Mayeux, P., and Bouscary, D. (2010). Perspectives on inhibiting mTOR as a future treatment strategy for hematological malignancies. Leukemia *24*, 1686–1699.

Chen, C., Liu, Y., Liu, R., Ikenoue, T., Guan, K.-L., Liu, Y., and Zheng, P. (2008). TSC-mTOR maintains quiescence and function of hematopoietic stem cells by repressing mitochondrial biogenesis and reactive oxygen species. J. Exp. Med. *205*, 2397–2408.

Choo, A.Y., Yoon, S.-O., Kim, S.G., Roux, P.P., and Blenis, J. (2008). Rapamycin differentially inhibits S6Ks and 4E-BP1 to mediate cell-type-specific repression of mRNA translation. Proc. Natl. Acad. Sci. USA *105*, 17414–17419.

Christensen, J.L., and Weissman, I.L. (2001). Flk-2 is a marker in hematopoietic stem cell differentiation: a simple method to isolate long-term stem cells. Proc. Natl. Acad. Sci. USA *98*, 14541–14546.

Fruman, D.A., Snapper, S.B., Yballe, C.M., Davidson, L., Yu, J.Y., Alt, F.W., and Cantley, L.C. (1999). Impaired B cell development and proliferation in absence of phosphoinositide 3-kinase p85alpha. Science *283*, 393–397.

Gan, B., Sahin, E., Jiang, S., Sanchez-Aguilera, A., Scott, K.L., Chin, L., Williams, D.A., Kwiatkowski, D.J., and DePinho, R.A. (2008). mTORC1-dependent and -independent regulation of stem cell renewal, differentiation, and mobilization. Proc. Natl. Acad. Sci. USA *105*, 19384–19389.

Guertin, D.A., Stevens, D.M., Thoreen, C.C., Burds, A.A., Kalaany, N.Y., Moffat, J., Brown, M., Fitzgerald, K.J., and Sabatini, D.M. (2006). Ablation in mice of the mTORC components raptor, rictor, or mLST8 reveals that mTORC2 is required for signaling to Akt-FOXO and PKCalpha, but not S6K1. Dev. Cell *11*, 859–871.

Hsu, P.P., Kang, S.A., Rameseder, J., Zhang, Y., Ottina, K.A., Lim, D., Peterson, T.R., Choi, Y., Gray, N.S., Yaffe, M.B., et al. (2011). The mTOR-regulated phosphoproteome reveals a mechanism of mTORC1-mediated inhibition of growth factor signaling. Science *332*, 1317–1322.

Janes, M.R., Limon, J.J., So, L., Chen, J., Lim, R.J., Chavez, M.A., Vu, C., Lilly, M.B., Mallya, S., Ong, S.T., et al. (2010). Effective and selective targeting of leukemia cells using a TORC1/2 kinase inhibitor. Nat. Med. *16*, 205–213.

Kalaitzidis, D., and Neel, B.G. (2008). Flow-cytometric phosphoprotein analysis reveals agonist and temporal differences in responses of murine hematopoietic stem/progenitor cells. PLoS ONE *3*, e3776.

Kharas, M.G., Okabe, R., Ganis, J.J., Gozo, M., Khandan, T., Paktinat, M., Gilliland, D.G., and Gritsman, K. (2010). Constitutively active AKT depletes hematopoietic stem cells and induces leukemia in mice. Blood *115*, 1406–1415.

Kiel, M.J., Yilmaz, O.H., Iwashita, T., Yilmaz, O.H., Terhorst, C., and Morrison, S.J. (2005). SLAM family receptors distinguish hematopoietic stem and progenitor cells and reveal endothelial niches for stem cells. Cell *121*, 1109–1121.

Kühn, R., Schwenk, F., Aguet, M., and Rajewsky, K. (1995). Inducible gene targeting in mice. Science *269*, 1427–1429.

Laplante, M., and Sabatini, D.M. (2012). mTOR signaling in growth control and disease. Cell *149*, 274–293.

Lee, J.Y., Nakada, D., Yilmaz, O.H., Tothova, Z., Joseph, N.M., Lim, M.S., Gilliland, D.G., and Morrison, S.J. (2010). mTOR activation induces tumor suppressors that inhibit leukemogenesis and deplete hematopoietic stem cells after *Pten* deletion. Cell Stem Cell *7*, 593–605.

Lo Celso, C., Fleming, H.E., Wu, J.W., Zhao, C.X., Miake-Lye, S., Fujisaki, J., Côté, D., Rowe, D.W., Lin, C.P., and Scadden, D.T. (2009). Live-animal tracking of individual haematopoietic stem/progenitor cells in their niche. Nature *457*, 92–96.

Magee, J.A., Ikenoue, T., Nakada, D., Lee, J.Y., Guan, K.-L., and Morrison, S.J. (2012). Temporal changes in PTEN and mTORC2 regulation of hematopoietic stem cell self-renewal and leukemia suppression. Cell Stem Cell *11*, this issue, 415–428.

Morita, Y., Ema, H., and Nakauchi, H. (2010). Heterogeneity and hierarchy within the most primitive hematopietic stem cell compartment. J. Exp. Med. *207*, 1178–1182.

Osawa, M., Hanada, K.-I., Hamada, H., and Nakauchi, H. (1996). Long-term lymphohematopoietic reconstitution by a single CD34-low/negative hematopoietic stem cell. Science *273*, 242–245.

Peterson, T.R., Sengupta, S.S., Harris, T.E., Carmack, A.E., Kang, S.A., Balderas, E., Guertin, D.A., Madden, K.L., Carpenter, A.E., Finck, B.N., and Sabatini, D.M. (2011). mTOR complex 1 regulates lipin 1 localization to control the SREBP pathway. Cell *146*, 408–420.

Pronk, C.J., Rossi, D.J., Månsson, R., Attema, J.L., Norddahl, G.L., Chan, C.K., Sigvardsson, M., Weissman, I.L., and Bryder, D. (2007). Elucidation of the phenotypic, functional, and molecular topography of a myeloerythroid progenitor cell hierarchy. Cell Stem Cell *1*, 428–442.

Qian, H., Buza-Vidas, N., Hyland, C.D., Jensen, C.T., Antonchuk, J., Månsson, R., Thoren, L.A., Ekblom, M., Alexander, W.S., and Jacobsen, S.E.W. (2007). Critical role of thrombopoietin in maintaining adult quiescent hematopoietic stem cells. Cell Stem Cell *1*, 671–684.

Ruzankin, Y., Pinzon-Guzman, C., Asare, A., Ong, T., Pontano, L., Cotsarelis, G., Zediak, V.P., Velez, M., Bhandoola, A., and Brown, E.J. (1997). Deletion of the developmentally essential gene ATR in adult mice leads to age-related phenotypes and stem cell loss. Cell Stem Cell *1*, 113–126.

Sarbassov, D.D., Ali, S.M., Sengupta, S., Sheen, J.-H., Hsu, P.P., Bagley, A.F., Markhard, A.L., and Sabatini, D.M. (2006). Prolonged rapamycin treatment inhibits mTORC2 assembly and Akt/PKB. Mol. Cell *22*, 159–168.

Sengupta, S., Peterson, T.R., Laplante, M., Oh, S., and Sabatini, D.M. (2010). mTORC1 controls fasting-induced ketogenesis and its modulation by ageing. Nature *468*, 1100–1104.

Shiota, C., Woo, J.T., Lindner, J., Shelton, K.D., and Magnuson, M.A. (2006). Multiallelic disruption of the rictor gene in mice reveals that mTOR complex 2 is essential for fetal growth and viability. Dev. Cell *11*, 583–589.

Sykes, S.M., Lane, S.W., Bullinger, L., Kalaitzidis, D., Yusuf, R., Saez, B., Ferraro, F., Mercier, F., Singh, H., Brumme, K.M., et al. (2011). AKT/FOXO signaling enforces reversible differentiation blockade in myeloid leukemias. Cell *146*, 697–708.

Tothova, Z., Kollipara, R., Huntly, B.J., Lee, B.H., Castrillon, D.H., Cullen, D.E., McDowell, E.P., Lazo-Kallanian, S., Williams, I.R., Sears, C., et al. (2007). FoxOs are critical mediators of hematopoietic stem cell resistance to physiologic oxidative stress. Cell *128*, 325–339.

Warr, M.R., Pietras, E.M., and Passegué, E. (2011). Mechanisms controlling hematopoietic stem cell functions during normal hematopoiesis and hematological malignancies. Wiley Interdiscip. Rev. Syst. Biol. Med. *3*, 681–701.

Yang, L., Bryder, D., Adolfsson, J., Nygren, J., Mansson, R., Sigvardsson, M., and Jacobsen, S.E. (1995). Identfication of $Lin^{-}Sca1^{+}kit^{+}CD34^{+}Flt3^{-}$ short-term hematopoietic stem cells capable of rapidly reconstituting and rescuing myeloablated transplant recipients. Blood *105*, 2717–2723.

Yilmaz, O.H., Valdez, R., Theisen, B.K., Guo, W., Ferguson, D.O., Wu, H., and Morrison, S.J. (2006). Pten dependence distinguishes haematopoietic stem cells from leukaemia-initiating cells. Nature *441*, 475–482.

Yu, Y., Yoon, S.O., Poulogiannis, G., Yang, Q., Ma, X.M., Villén, J., Kubica, N., Hoffman, G.R., Cantley, L.C., Gygi, S.P., and Blenis, J. (2011). Phosphoproteomic analysis identifies Grb10 as an mTORC1 substrate that negatively regulates insulin signaling. Science *332*, 1322–1326.

Zhang, J., Grindley, J.C., Yin, T., Jayasinghe, S., He, X.C., Ross, J.T., Haug, J.S., Rupp, D., Porter-Westpfahl, K.S., Wiedemann, L.M., et al. (2006). PTEN maintains haematopoietic stem cells and acts in lineage choice and leukaemia prevention. Nature *441*, 518–522.

Zheng, J., Umikawa, M., Zhang, S., Huynh, H., Silvany, R., Chen, B.P.C., Chen, L., and Zhang, C.C. (2011). Ex vivo expanded hematopoietic stem cells overcome the MHC barrier in allogeneic transplantation. Cell Stem Cell *9*, 119–130.